



## Original Research Article

### ADSORPTION STUDY ON THE REMOVAL OF CU (II) IONS FROM AQUEOUS SOLUTION USING MELON (*CITRUS COCOLYNTHUS*) HUSK AS A BIOSORBENT IN A FIXED BED COLUMN

<sup>1</sup>\*Yahya, M.D., <sup>2</sup>Suleiman, B., <sup>3</sup>Iyaka, Y.A., <sup>1</sup>Saliu, H. and <sup>2</sup>Garba, U.

<sup>1</sup>Department of Chemical Engineering, School of Engineering and Engineering Technology, Federal University of Technology Minna, PMB 65, Niger State, Nigeria

<sup>2</sup>Department of Chemical Engineering, School of Engineering and Environmental Design, Usmanu Danfodiyo University Sokoto, Sokoto State, Nigeria

<sup>3</sup>Department of Chemistry, Federal University of Technology, Minna, Nigeria.

\*muibat.yahya@futminna.edu.ng

#### ARTICLE INFORMATION

##### Article history:

Received 18 May, 2018

Revised 27 June, 2018

Accepted 29 June, 2018

Available online 30 June, 2018

##### Keywords:

Fixed bed column

Cu (II) ions removal

Melon husk

Adsorption

Breakthrough curves

Aqueous solution

#### ABSTRACT

*Adsorption potentials of melon husk for the removal of copper (II) ions from aqueous solution in a fixed bed column was investigated. Melon husk was prepared and characterized based on functional groups and morphology using Fourier Transform Infra Red (FTIR) spectrum and Scanning Electron Microscope (SEM) imaging respectively. Fixed bed column study was carried out as a function of simulated effluent flow rate (0.5-1.5 ml/min), initial Cu (II) concentration (5-20 mg/l) and bed height (6-12 cm). The dynamics of the bed was correlated using kinetics isotherms, Adams-Bohart, Bed Depth Service Time (BDST) and Yoon Nelson models. The SEM morphology indicated the adsorbent's high surface roughness that is evenly dispersed before adsorption and lower adsorbent porosity after adsorption. FTIR spectrum of the adsorbent before and after adsorption showed peaks with slight shifts in the position of carboxylic (1682.92-1670.91  $\text{cm}^{-1}$ ) and amine (1615.86-1560.15  $\text{cm}^{-1}$ ) groups attributed to the attachment of Cu (II) ions via functional groups. The BDST model gave the best agreement between the experimental and the model prediction with  $R^2 = 0.991$ . High metal removal (87.5-100%) was achieved within the range of chosen variables. The column performance indicated the efficiency of melon husk as an adsorbent for Cu (II) which can be utilised in waste water treatment.*

© 2018 RJEES. All rights reserved.

## 1. INTRODUCTION

The present level of environmental pollution through air, land and water sources (streams, lakes, underground and oceans) by substances considered to be a threat for continuous existence of living

organisms is alarming (Daniel *et al.*, 2014; Ahmad *et al.*, 2016). These substances can either be contaminants in the form of pathogens, sediments, heavy metals and microorganisms. Plants and animals cannot survive in any water that is fully contaminated with these harmful toxic substances. At very extreme circumstances, contamination of water bodies can lead to the death of a large number of aquatic life such as plants, fishes, animals and consequently, human beings (Nwankwo, 2007; Martin-Lara *et al.*, 2016; Markou *et al.*, 2016).

Numerous methods have been developed for the treatment of contaminated water such as precipitation, ion exchange, electrochemical treatment, membrane separation, ultra-filtration, phyto-remediation, reverse osmosis and adsorption (Panda *et al.*, 2007; Blanes *et al.*, 2016; Taty-Costodes *et al.*, 2005; Alyüz and Veli, 2009). The use of commercial activated carbon has been widely explored in the field of adsorption. Although, it's high cost still remains as its limitation. In recent years, the need for an effective, sustainable and affordable method to remove heavy metals from contaminated water has drawn serious research attention to develop new methods that are efficient and less expensive in comparison to the commercially available activated carbon (Sivakumar and Palanisamy, 2009; Amirnia *et al.*, 2016). Some research efforts such as the use of the biosorption process had succeeded in exploring new technologies for the removal of toxic metals from waste water (Taty-Costodes *et al.*, 2005; Amirnia *et al.*, 2016; Malkoc and Nuhoglu, 2006). There has been a drastic shift to biosorption as a promising method due to the vast availability of various biological biomasses in addition to their respective metal binding capacities (Muhammad *et al.*, 2011; Ahmad *et al.*, 2016). Biosorption has provided an enticing alternative to other physio-chemical methods that has been explored as a means of heavy metal removal (Chaundry and Ijiaz, 2014). It is a phenomenon in which certain biological materials tend to accumulate contaminants such as heavy metals from wastewater via the metabolically mediated or physio-chemical pathways of uptake (Chaundry and Ijiaz, 2014).

Numerous studies have been carried out and documented in the field of biosorption which were mainly based on the use of agro-based adsorbents characterized by low cost and established potentials for the heavy metals removal from waste water. The feasibility of using agro-based material as an adsorbent depends on its ease of operation, effectiveness, selectivity with a robust capacity and availability as a raw material in abundance (Chaundry and Ijiaz, 2014). A significant number of Agro waste have been explored as adsorbents (Abdolali *et al.*, 2016) such as the sugarcane bagasse (Gupta, 2003), spent tea leaves (Malkoc *et al.*, 2006), palm nuts shell (Nwabanne and Igbokwe 2012), pea nuts (Watwoyo and Marshall (1999), rice husks (Zulkali *et al.*, 2006; Asadi *et al.*, 2008), saw dusts (Ajmal *et al.*, 1998; Malkoc *et al.*, 2006), melon peel and husks (Daniel *et al.*, 2014; Babarinde and Omisore, 2014) and so on.

Melon husk is readily available across Nigeria especially in Kogi State, North central part of the country. The state has about 211, 600 hectares of land being utilized for the cultivation of melon (Sunday *et al.*, 2012). The use of melon seed husk as an adsorbent for heavy metal removal can lower problems associated with the deposition of toxic effluents into the environment and increase economic gain to industries. It also reduces the pollution level generated by the husk, thereby converting waste to wealth: a benefit to be derived by melon traders and the general public.

Nwankwo (2007) reported the use melon (*Citrullus colocynthis*) husk activated with sulphuric acid ( $H_2SO_4$ ), sodium hydroxide and urea as an adsorbent in the removal of lead (II) and cadmium (II) from industrial effluents. Djelloul and Hamdaoui (2004) conducted batch studies and dynamic studies in the removal of methylene blue using melon peel (husk) in packed bed column. Batch adsorption studies for the removal of lead by saponified melon peel has also been reported by Chaundry and Ijiaz (2014). Chellam *et al.* (2014) studied the adsorption of Cadmium (II) on *Cucumis* melon peel. Babarinde and Omisore (2014) reported the application of kinetic, isothermal and thermodynamic models in the study of Cd (II), Zn (II) and Pb (II) adsorption on melon husk. It is evident from previous reported studies that adsorption of Copper (II) ion using melon husk as adsorbent in a fixed bed column has not been investigated and this thus necessitated this research to serve as a knowledge-based record for its utilization in wastewater treatment.

## 2. MATERIALS AND METHODS

### 2.1. Materials Collection and Preparation of Adsorbent

Melon husks used in this study were collected from a shelling centre in Bida Local Government area of Niger State, Nigeria. Interfering particles such as debris and stones were handpicked from the melon husks after which it was washed severally with tap water and further rinsed with distilled water. The husks were dried in an oven at a temperature of 80°C for 12 hours. The moisture content of the husk was determined by weighing it before and after drying. The resulting dried husks were pulverised using an electric blender (Moulinex) and sieved using a rotary shaker (Octagon 2000, Endecotts England) to obtain dried and pulverised melon husk particles of size 350 µm which was used as the adsorbent.

### 2.2. Experimental Set Up

Fixed bed column studies were carried out using a glass column of 2.76 cm internal diameter and 30cm length. Grinded melon husk of particle size 350 µm was used. The melon husks were packed to a height of 6 cm in the column with a perforated parking at the bottom. Diluted solution of the Copper (II) solution of initial concentration 5mg/l was continuously fed in the downward direction into the column at a flow rate of 0.5 ml/min with the aid of a peristaltic pump (Longer BQ50-1J). At different pre-defined intervals, samples were collected in sample bottles and measured for residual concentration using a Flame Atomic Absorption Spectrophotometer (Varian SpectrAA 220FS). Adsorption parameters were evaluated such as initial metal ion concentration, bed height and flow rate at various conditions for a period of 40 hours after which the column study with respect to each parameter were determined. The melon husks used for each experimental run were weighed before being fed into the column, removed after the adsorption and then dried in an oven.

### 2.3. Effect of Initial Metal Ion Concentration

Three different concentrations of Cu (II) ions of 5, 10 and 20 mg/L were used as influents to study the suitability of melon husks in the removal of Cu (II) ions. A constant flow rate of 0.5 ml/min at bed depth of 6 cm was maintained during the experiment and the effluent was collected at pre-determined intervals to measure the residual ion concentrations.

### 2.4. Effect of Flow Rate

Since the contact period between the Cu (II) ions and the melon husks surface is directly influenced by the rate of flow of the influent, in this study, the flow rate of influent of Cu (II) was varied at 0.5, 1.0 and 1.5 ml/min. Throughout the experiment, the initial Cu (II) ions concentration and bed height was maintained as 5 mg/L and 6 cm respectively. The resulting effluent was collected at pre-determined intervals to measure the residual Cu (II) ions concentration.

### 2.5. Effect of the Bed Height

To evaluate the effect of the bed height, different amounts of melon husks were filled into three (3) separate columns up to a height of 6, 8 and 12cm. An initial concentration of Cu (II) ions at 5 mg/L was fed into the columns separately at constant flow rate of 0.5ml/min. At different pre-determined intervals, the effluent was collected for residual Cu (II) ions analysis.

### 2.6. Modeling of Column Dynamic Behaviour

The kinetic isotherms used were: Adams-Bohart, BDST, and Yoon Nelson models reported by Blanes *et al.* (2016), Sivakumar and Palanisamy (2009) and Chowdhury *et al.* (2013) and ascertained to be adequate in

the prediction of the behavior of fixed bed dynamic adsorption columns were used in this study. The three models provided the data required for the efficient design of the fixed column at optimal conditions.

### 2.6.1. Adams-Bohart model

Equations (1) and (2) show the Adams Bohart basic equations that describes the relationship between the ratios of the effluent concentration to the initial metal ion concentration ( $C_e/C_0$ ) with time  $t$ . This model is used for the analysis and estimation of the initial section of the breakthrough curve.

$$\frac{C_e}{C_0} = \exp(k_{AB}C_0t - k_{AB}N_0\frac{u}{U_0}) \quad (1)$$

Where  $k$  is the kinetic constant (l/mg hr);  $U_0$  is the linear flow rate (cm/hr) defined as the ratio of the flow rate  $Q$  (ml/hr) to the cross-sectional area  $A$  (cm<sup>2</sup>) and  $N_0$  is the saturation concentration (mg/l). When Equation (1) is linearized, the model parameters can be evaluated from the slope and intercepts of a linear plot of  $\ln(C_e/C_0)$  versus  $t$ .

The linearized form is expressed as:

$$\ln\frac{C_e}{C_0} = k_{AB}C_0t - k_{AB}N_0\frac{Z}{U_0} \quad (2)$$

The linear graph obtained from a plot of  $\ln(C_e/C_0)$  against time gives  $k_{AB}C_0$  as its slope and  $N_0$  as the intercept. The values of  $k_{AB}$  and  $N_0$  determined alongside other parameters were used to determine new  $C_e/C_0$  values predicted from the model Equation (2). The experimental ratio of  $C_e/C_0$  and those predicted from Adam's Bohart model equations were determined while studying the effects of flow rate, bed height and initial concentration.

### 2.6.2. Bed depth service time (BDST) model

The BDST model predicts the relationship between bed heights and service time  $t$  as reported by Blanes *et al.* (2016) and Vijayaraghavan and Yun (2008). The model states that the bed height and service time of a column bear a linear relationship as given in the BDST model expression in Equation (3).

$$\ln\left(\frac{C_0}{C_B}\right) = \ln\left(\exp\left[\frac{N_0KX}{u}\right] - 1\right) - KC_0t \quad (3)$$

Linearized form of Equation (3) is given as Equation (4).

$$t = \frac{N_0}{uC_0}X - \frac{1}{KC_0}\ln\left(\frac{C_0}{C_B} - 1\right) \quad (4)$$

Where  $C_B$  is the desired concentration (mg/l) of solute at breakthrough,  $K$  is the adsorption rate constant (L mg<sup>-1</sup> min<sup>-1</sup>), and the remaining symbols have their usual meanings.

### 2.6.3 Yoon Nelson model

Equation (5) and (6) give the basic expression for the Yoon Nelson Model. The principle of operation is based on the consideration that the rate at which the probability of sorption of each molecule decreases is proportional to the probability of sorbate sorption and breakthrough on the sorbent. The mathematical statement of this model is expressed by Equation (5).

$$\frac{C_e}{C_0 - C_e} = \exp(k_{YN}t - \tau k_{YN}) \quad (5)$$

$k_{YN}$  and  $\tau$  are the rate constant ( $\text{min}^{-1}$ ) and the time in minutes required for 50 % adsorbate breakthrough respectively. The linearized form of Equation (5) is given as Equation (6).

$$\ln \frac{C_e}{C_0 - C_e} = k_{YN}t - k_{YN}\tau \quad (6)$$

The symmetrical nature of the breakthrough curves is that the amount of adsorbate that is adsorbed in a fixed bed column is half of the total adsorbate entering into the adsorption bed within a period of  $2\tau$ .

The adsorption capacity of a given bed is evaluated using Equation (7).

$$q_0 = \frac{q_{total}}{w} = \frac{\frac{1}{2}C_0[(Q/1000)(2\tau)]}{w} = \frac{C_0 Q\tau}{1000w} \quad (7)$$

Values of the ratio ( $C_e/C_0$ ) predicted from the Yoon Nelson model parameters were determined and the effect of flow rate, bed height and initial concentration on the Yoon Nelson model parameters studied.

### 3. RESULTS AND DISCUSSION

#### 3.1. Characterization of Adsorbent

##### 3.1.1. Scanning electron microscope (SEM) micrographs

SEM was used to study the adsorbent's surface morphology and to derive relevant deductions on the extent of interaction between components of the melon husks and the Cu (II) ions in the adsorption process. The textural structure of the adsorbent before and after adsorption of Cu (II) ions is presented as scanning electron micrographs in Figures 1 and 2 respectively. The surface roughness observed in Figure 1 is high, having heterogeneous cavities and pore, an indication that the adsorbent has high surface area as reported in a previous study by Djelloul and Hamdaoui (2014). The high rough surface observed suggests high probability for the Cu (II) ions to be locked in and adsorbed as also observed and reported in the work of Zhang *et al.* (2011) that used rice husk carbons in the removal of Cu (II) from aqueous solution. In related studies on melon husk and *Cucumis melon* peel adsorbents reported by Giwa *et al.* (2013) and Chellam *et al.* (2014), similar observations of good surface roughness and the presence of pore sites on the adsorbents was observed. The SEM result after adsorption shows that there were fewer number of pores left after adsorption process in comparison to the images of the raw melon husks before adsorption, an indication of Cu (II) ions captured by the fresh adsorbent pores leading to the reduction in the number of pore sites available for the adsorption process.

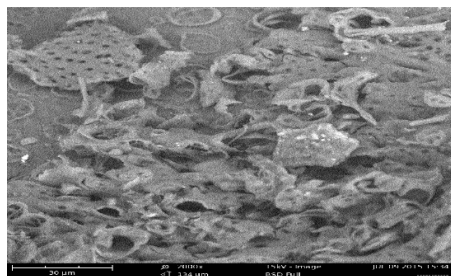


Figure 1: SEM Images (2000 ×) for Melon husks before adsorption

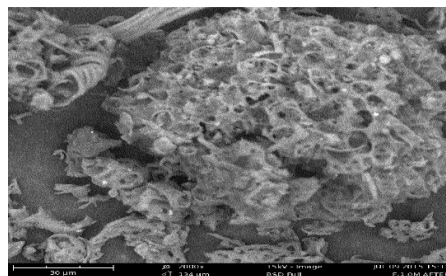


Figure 2: SEM Images (2000 ×) for melon husks after adsorption

### 3.1.2. Fourier-transform infrared (FT-IR) spectra

FTIR spectra of the melon husk before and after adsorption were recorded on the FTIR spectrophotometer plotted as a percentage of transmittance versus wave number in the range 400 to 4000  $\text{cm}^{-1}$  at room temperature. The FT-IR spectra of raw and Cu(II) ion loaded biomass of melon husk were measured in order to obtain information on the nature of possible interactions between the functional groups present on the surface of the melon husk and the Cu (II) ions. The spectra in Figures 3 and 4 show various functional groups which explain the complexity of the adsorbent material. It can be observed that the broad and distinguished peak of the spectrum of melon seed husk displayed in between (3544.21  $\text{cm}^{-1}$  3617.24  $\text{cm}^{-1}$ ) is due to overlapping stretching vibration of O-H of alcohols and N-H of amines (Mousumi *et al.*, 2017). This could be as result of an inter-molecular hydrogen bonding of polymeric compounds such as phenols and carboxylic acid; as in pectin, cellulose groups on the adsorbent surface (Saeedeh *et al.*, 2014). The peak band at 2922.94  $\text{cm}^{-1}$  may be attributed to the -CH stretching vibration of methyl and methoxy group (Reddy *et al.*, 2014; Kausar *et al.*, 2016). The peak at 1682.92  $\text{cm}^{-1}$  corresponds to the -C=O stretching of carboxylic acid or esters (Blanes *et al.*, 2016). A broad peak observed at 1520.60  $\text{cm}^{-1}$  shows the presence of C-H stretching of aldehydes (Kausar *et al.*, 2016). The sharp peak at 1376.56  $\text{cm}^{-1}$  may be attributed to the -CH<sub>3</sub> groups (Ghasemi *et al.*, 2013). Presence of phenolic C-O and O-H group can be assigned to the peak at 1271.71  $\text{cm}^{-1}$  (Basu *et al.*, 2017). The intensities at 721.96  $\text{cm}^{-1}$ , 469  $\text{cm}^{-1}$  and 418.91  $\text{cm}^{-1}$  indicates the out of plane O-H, N-O and C-H functional groups (Foo and Hameed., 2012).

Figure 4 shows the FT-IR spectra of the melon seed husk obtained after adsorption of copper (ii) ions. The broad peak at 3338.2  $\text{cm}^{-1}$  represents the stretching of -OH bond due to the sorption of Cu (II) ions (Basu *et al.*, 2017). The broad band at 2725.31  $\text{cm}^{-1}$  to 1670.9  $\text{cm}^{-1}$  suggest the C-H, C=O and C-N group involvement (Kasuar *et al.*, 2017). The intense and broad band at around 1560.15  $\text{cm}^{-1}$  and 1376.56  $\text{cm}^{-1}$  can be assigned to the aromatic C=C, C-OH and C-C functional group (Choong *et al.*, 2018). The band from 1376.56  $\text{cm}^{-1}$  to 1459.1  $\text{cm}^{-1}$  represents the asymmetric and symmetric C-H stretching (Choong *et al.*, 2018). The peaks at 721.96  $\text{cm}^{-1}$  and 418.91  $\text{cm}^{-1}$  correspond to the stretching of C-O and C-C bond in both rings (Choong *et al.*, 2018). It is evident that after adsorption, more complex number of absorption peaks was present and a shift in the peak position of some functional groups such as for carboxylic (C=O) and amine (N-H) can be attributed to the attachment of Cu (II) ions to the adsorbent via the functional groups.

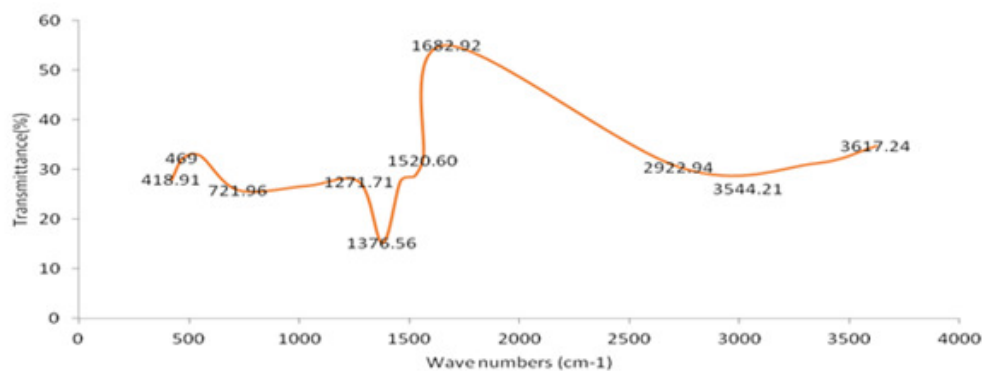


Figure 3: FT-IR spectra of melon husk before adsorption of Cu (II) ion

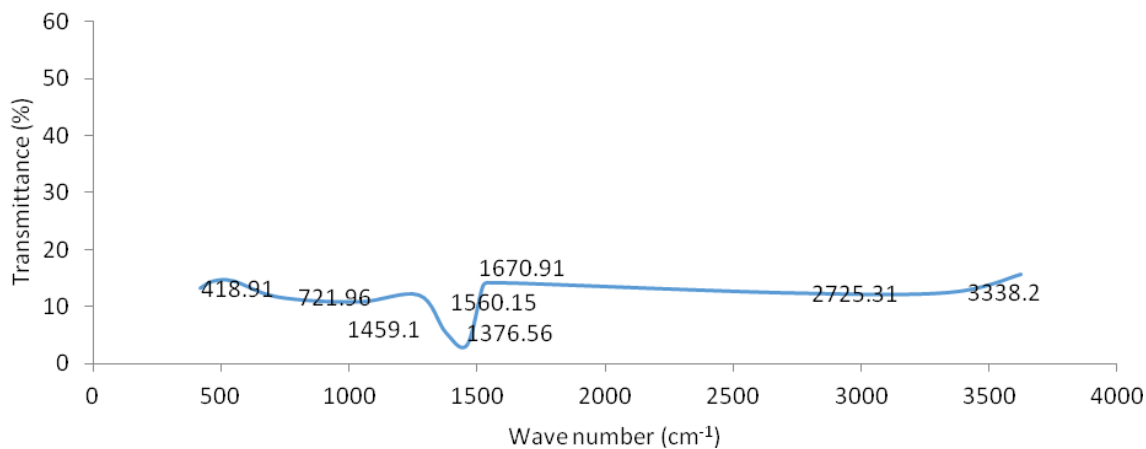


Figure 4: FT-IR spectra of melon husk after adsorption of Cu (II) ion

### 3.2. Effect of Operating Parameters on The Adsorption Of Cu (II) Ions

The result presented in Figures 5 to 7 and Table 1 shows the effect of operating variables studied in this work. The parameters investigated include flow rate, bed height and initial concentration of the solution which have been reported to have significant effect on heavy metals adsorption such as saw dust (Taty-Costodes *et al.*, 2005), waste tea (Malkoc and Nuhoglu, 2006), rice husk (Zhang *et al.*, 2011), Wong *et al.*, 2003), melon peel (Sunday *et al.*, 2012; Barinde *et al.*, 2014;), maize tassel (Shekhula *et al.*, 2012) and seaweed (Lodeiro *et al.*, 2006). Breakthrough curves behaviour was monitored to study these effects. The amount of copper (II) ion adsorbed for each time interval was determined in accordance with procedure reported by Nasehir *et al.* (2011).

#### 3.2.1. Effect of flow rate

Figure 5 shows the effect of flow rate on the Cu (II) adsorption by a raw melon husk at constant initial concentration and bed height of 5 mg/l and 6 cm respectively. The flow rate was varied from 0.5 to 1.5 ml/min. Careful observation of the breakthrough curve in Figure 5 shows that the adsorbent was not saturated after 2400 minutes of flow of the solution through the column within the given range of flow rates investigated. This showed that the melon husk has high porosity and longer time would be taken before the bed can be exhausted. This is a positive attribute as fixed bed with shorter time indicate early bed saturation and frequency in the changing of the adsorbent. Invariably breakthrough was not achieved at the evaluated time interval.

The effluent concentrations at the end of time of flow for the different flow rate studied were observed to be at equilibrium. Equilibrium was achieved faster as the flow rate of the inlet concentration increases. Table 1 shows that total throughput volume increases from 734.5 ml to 1566 ml as the flow rate decreases from 1.5 ml/min to 1.0 ml/min. Meanwhile, at 0.5 ml/min, a throughput of 2900 ml was recorded. This means, on the average there was about 50 % throughput decrease for any 0.5 ml/min increase in flow rate. This indicates that at lower flow rate, the adsorption proceeds rapidly since the adsorption sites are able to properly capture Cu (II) ions. It was further observed that the maximum sorption capacity, percentage (%) metal removal and equilibrium uptake decreased as the flow rate increased as reported by Amirmia *et al.*, (2016). The decrease in these measures of column performance was a proportional increase. The low percent metal removal at higher flow rate (1.5 ml/min) considered can be linked to the short residence time for the solute to interact with the surface of the sorbent and diffuse into the pores of the sorbent causing solute to leave before equilibrium is achieved (Abdolali *et al.*, 2016). More importantly, the biosorbent gets saturated easily at

early stage due to shorter contact time, large amounts of adsorbed ions and weak distribution of the liquid within the column resulting into lower solute diffusivity into the biosorbent as also observed by (Taty-Costodes *et al.*, 2005; Amirnia *et al.*, 2016). Generally, there was decrease in percent metal removal as the flow rate increases as shown in Table 1. In addition, at higher flow rate particles adsorbed can equally fall out thereby reducing adsorption efficiency.

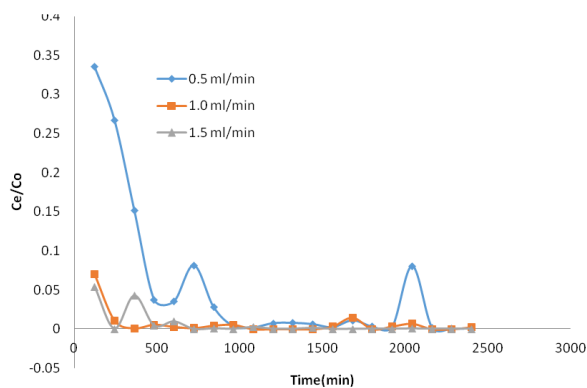


Figure 5: Breakthrough curve showing the effect of different flow rates at bed height of  $Z=6$  cm and Initial concentration= $5$  mg/l on the adsorption of Cu (II) onto raw melon husk

### 3.2.2. Effect of bed height

As reported by Malkoc and Nuhoglu (2006), the amount of metals retained as accumulation in a fixed bed column has largely been associated to the sorbent quantity available in the column. The higher the bed height the more reaction sites to accommodate the adsorbing metals. Therefore, different bed heights constitute different amounts of sorbents in the column. Three different breakthrough curves measured at various bed heights (6, 8 and 12 cm), constant flow rate and initial concentration of copper (II) solution shows that the effluent concentration was at equilibrium at the end of total flow time (2400 minutes) as shown in Figure 6. Thus, saturation was not achieved as such conclusion cannot be drawn at this stage on the optimal bed height that gives the best column performance. However, this provides insight on how increase in the bed height can affects the column performance. The sorption capacity and percentage metal removal increased as the bed height increases. The Figure also shows that the throughput volume increases from 2200 to 2900 ml when bed height increases from 6 to 12 cm. This is because a bigger bed height provides more adsorbent mass and invariably means more surface area leading to an increased volume of treated solution. This is in agreement with the findings reported by Saad *et al.* (2015) in a related study on the removal of uranium by phosphonated cross-linked polyethylenimine.

Further analysis of the result in Table 1 has shown that at maximum bed height of 12 cm considered, 100 % total metal removal was achieved indicating that further removal could be achieved since more sorption sites are more likely available for the metal ions adsorption. Furthermore, the effect of bed height as shown in Table 1 appears to have a pronounce contribution to the column performance efficiency.

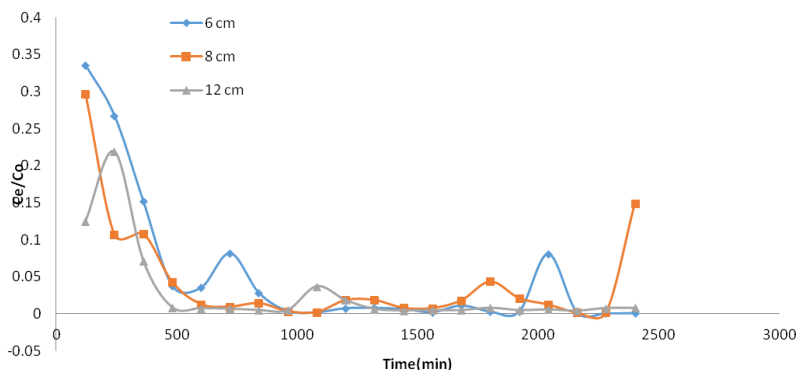


Figure 6: Breakthrough curve showing the effect of different bed heights at flowrate  $Q = 0.5$  ml/min and Initial concentration  $C_0 = 5$  mg/l on the adsorption of Cu (II) onto raw melon husk

### 3.2.3. Effect of initial Cu (II) concentration

Breakthrough curve is greatly affected by an increase in initial metal concentration at constant flow rate and bed height experimental conditions (Amirnia et al., (2016); Malkoc and Nuhoglu (2006)). The effect of initial concentration (5, 10 and 20 mg/l) of influent copper solution on the adsorption of Cu (II) by raw melon husk at constant bed height of 6 cm and flow rate of 0.5 ml/min was investigated. The results obtained as presented in Figure 7 shows the breakthrough curve for the effect of different initial concentrations on the adsorption of Cu (II). It was observed that for all initial concentrations of influent solution studied, the concentration ( $C_e$ ) of copper (II) ion in the effluent solution was at equilibrium within the total flow time (2400 minutes) considered. The reason for this can be linked to the inability of the bed to reach breakthrough/saturation as a result of complete removal of the Cu (II) even beyond 2400 minutes. Though breakthrough was not reached but literature has shown that adsorbents are exhausted faster at higher initial concentrations leading to early appearance of breakthrough due to quick adsorbents sites saturation and lower treated volume (Malkoc and Nuhoglu 2006; Saad *et al.*, 2015). The reverse is the case when using lower initial concentration (5 mg/l). It was observed that there was an increase in the treated volume of the solution as a result of lower concentration gradient which was responsible for a very slow transport and decrease in the coefficient of mass transfer or diffusion (Saad *et al.*, 2015; Amirnia and Margaritis 2016.) Table 1 shows that increase in  $C_0$  from 5 to 20 mg/l caused a corresponding increase in bed sorption capacity from 5.679 to 23.248 mg/g which was the highest uptake. The high uptake is as a result of high concentration difference between the Cu (II) ion on the melon husk and that in the solution.

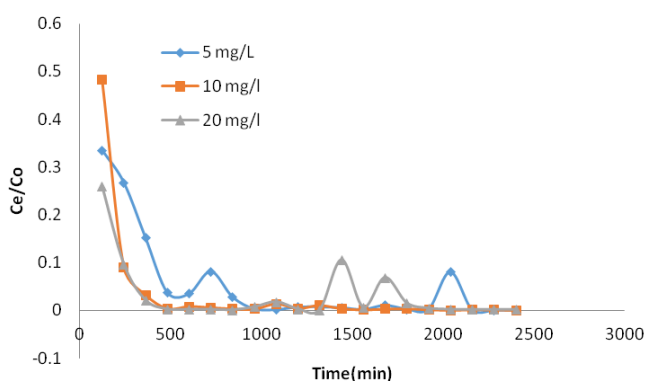


Figure 7: Breakthrough curve showing the effect of different initial concentrations at flow rate of 0.5 ml/min and bed height of 6 cm on the adsorption of copper (II) onto raw melon.

Table 1: Data of column parameters at different inlet Cu (II) concentration, bed heights and flow rates

Flow rate Q(ml/min)	Bed height Z(cm)	Inlet concentration C <sub>0</sub> (mg/l)	Treated volume (ml)	Max sorption capacity q <sub>total</sub> (mg)	Equilibrium uptake q <sub>eq(exp)</sub> (mg/g)	Total percent removal (%)
0.5	6	5	2200	17.036	0.761	94.64
1.0	6	5	1566	11.357	0.747	94.62
1.5	6	5	734.5	05.679	0.352	91.62
0.5	8	5	2593	20.710	1.494	98.62
0.5	12	5	2900	21.980	1.784	100.0
0.5	6	10	844	20.189	1.142	100.0
0.5	6	20	690	23.248	1.491	96.87

### 3.4. Analysis of Fixed Bed Breakthrough Models

Modelling of the dynamics of fixed bed adsorption process was studied via the applications of three different models namely the Adams Bohart model, Bed depth service time (BDST) and Yoon Nelson models. The influence of all the operating parameters (bed height, initial concentration and flow rate) was considered in the model study.

#### 3.4.1. Break through curve modelling with Adams-bohart model

Adams-Bohart model has been used to model several experimental data for a fixed bed sorption process and it is applied usually to describe the early stage of the breakthrough curves (Shekhula *et al.*, 2012). The model parameters were determined and comparison between experimental and theoretical Adams-Bohart breakthrough curves has been made and presented in Table 2 with the correlation coefficients showing how well the experimental data fits into the Adams-Bohart model. The breakthrough plots of the experimental and predicted values of ( $C_e/C_0$ ) versus time (minutes) at bed heights of 6, 8 and 12 cm were investigated at constant flow rate and initial concentration of 0.5 ml/min and 5 mg/l respectively. The Adams-Bohart model parameters determined are the Adams Bohart constant ( $k_{AB}$ ) and Sorption capacity ( $N_0$ ) determined from the slopes and intercepts of the linear plots of  $\ln(C_e/C_0)$  versus time (minutes). It was observed in Table 2 that rate constant  $k_{AB}$ , decreases with increase in bed heights from -0.00016 ml/mg.min at 6 cm to -0.00022 ml/mg.min at 12 cm. Sorption capacity ( $N_0$ ) also decreases from 6.022 mg/l at 6 cm to 2.3152 mg/l at 12 cm.

Table 2: Adams Bohart model constants for the adsorption of Cu (II) on raw melon husk in a fixed bed column

Q(ml/min)	L(cm)	Co (mg/l)	No(mg/l)	K <sub>AB</sub> (ml/ming)	R <sup>2</sup>
0.5	6	5	6.0220	-0.00016	0.1691
0.5	8	5	4.5162	-0.00016	0.1691
0.5	12	5	2.3152	-0.00022	0.4029
1.0	6	5	52.939	-0.00006	0.0416
1.5	6	5	11.574	-0.00034	0.1913
0.5	6	10	5.5837	-0.00017	0.6439
0.5	6	20	26.802	-0.00005	0.1505

Though, the stage at which these parameters were obtained, the bed was not saturated and breakthrough was not achieved. However, there was sudden decrease and increase in the rate  $k_{AB}$  when the concentration and flow rate increases. The absence of definite trend in the model parameters can be linked to the absence of breakthrough appearance within the period of this study indicating that the bed was not saturated. Therefore, the result indicates a poor description of the early stage of the breakthrough curve by this model characterized by low correlation coefficient in the range 0.1691 to 0.4029. In a related study in which breakthrough was achieved by Ushakumary and Madhu (2014) in the removal of Zinc (II) using *Alisma Plantago Aquatica*,  $k_{AB}$  and  $N_0$  increases from 0.00303 l/mg.min at 3 ml/min to 0.00439 l/mg.min at 6 ml/min. Meanwhile,  $N_0$  increases from 533.42 mg/l to 695.60 mg/l. The model did not fit well and poorly described the breakthrough

within the period examined having a maximum correlation coefficient of 0.6439 at a flow rate, bed height and initial concentration of 0.5, 6cm and 10 mg/l respectively

### 3.4.2. Break through curve modelling with Yoon-Nelson model

A linear plot of  $\ln[C_t/(C_0 - C_t)]$  against sampling time determines the values of  $\tau$  and  $k_{YN}$  from the intercept and slope of the plot of varying parameters against time. The values of  $k_{YN}$ ,  $\tau$ , and  $q_0$  were obtained and are listed in Table 3 where  $q_0 = C_0\theta\tau$  given that  $\theta$  is the solute flow rate. From the results obtained, it can be seen that the constant  $k_{YN}$  increases with increase in bed height from 6cm to 8cm and decreases from 8cm to 12 cm. It also fluctuated as the flow rate increased but increases uniformly with an increase in initial concentration as reported in previous study by Yahya *et al.* (2013). The rate constant  $k_{YN}$  has been reported to increase with increase in flow rate, bed height and inlet ion concentration in a previous study using oil palm fibre to remove Lead (II) by Nwabanne and Igbokwe (2012). There was an increase in  $\tau$  as bed height and initial concentration increases but a fluctuation in  $\tau$  was observed when flow rate was increased. However,  $q_0$  (mg/g) increases generally with increase in bed height and initial metal concentration but fluctuation was observed with respect to flow rate. The fluctuation in model parameters observed with respect to flow rate is a clear indication of the absence of bed saturation and fall out of the metal ions not properly attached to the adsorbent surface before the breakthrough. The absence of breakthrough observed over the period studied shows the potentials of the melon husk as an adsorbent of Cu (II) ion in solution. The result of correlation coefficient is generally low as shown in Table 3 an indication that the model did not describe the breakthrough curve adequately prior to the bed saturation state within the variation of all the operating variables studied for an adsorption period of 2400 minutes used.

Table 3: Yoon-Nelson model constants for the adsorption of Cu (II) on raw melon husk in a fixed bed column

Q(ml/min)	L(cm)	Co (mg/l)	$\tau$ (min)	$K_{yn}$	$q_0$ (mg/g)	$R^2$
0.5	6	5	732	-0.0022	1830	0.6166
0.5	8	5	3292	-0.0009	8230	0.1715
0.5	12	5	4407	-0.0011	11017.5	0.0886
1.0	6	5	4407	-0.0011	22035	0.0886
1.5	6	5	2397	-0.0017	17977.5	0.1931
0.5	6	10	1557	-0.0018	7785	0.6189
0.5	6	20	3678	-0.0010	36780	0.1540

### 3.4.3. Break through curve modelling with BDST model

The BDST is a model which predicts the relationship between service time and bed depth. The model states that there is a linear relationship between the bed height and service time of a column and tries to predict this relationship. The BDST parameters presented in Table 4 shows that the rate constant evaluated as the intercept of the BDST plot in Figure 8 characterizes the rate of transfer of the solute from the liquid to solid phase. It was also observed that service time increases with increase in bed height from a service time of 1320 min at bed height of 6 cm to a service time of 1800 min at a bed height of 12 cm. Rate constant  $K$  was obtained as  $0.001 \text{ L mg}^{-1} \text{ min}^{-1}$  and  $0.1153 \text{ mg/l}$  was obtained as the bed sorption capacity ( $N_0$ ). The bed sorption capacity predicts the bed of the column performance as the initial concentration changes. Increase in bed depth results into increase in residence time that provides a greater opportunity for the adsorbate molecules diffusion into the adsorbent, thereby leading to change in the capacity of the bed with service time. Kanadasan *et al.* (2010) studied the removal of methylene blue by palm oil mill effluent waste activated carbon and obtained a rate constant and bed sorption capacity of  $0.0112 \text{ l/ mg}^{-1} \text{ hr}^{-1}$  and  $1443 \text{ mg/l}$  respectively. A very large constant  $K_a$  means that a short bed can avoid breakthrough and the reverse is the case as reported by Malkoc and Nuhoglu (2006). High values of correlation coefficient ( $R^2=0.991$ ) shown in Figure 7 signified the high linearity between the bed height and service time. This indicates the reliability of the BDST model when applied to the fixed bed column study and the model parameters are reliable in the process scale up at different range of flow rates and initial metal concentration.

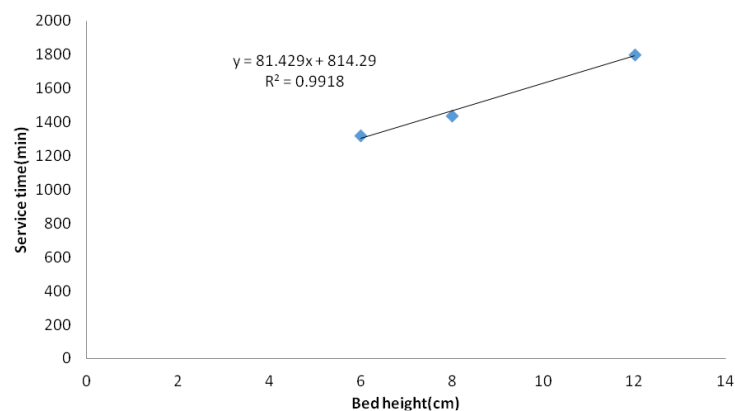


Figure 8: BDST model plot for Cu (II) biosorption by melon husk (flow rate = 0.5 ml/min, initial Cu (II) concentration = 5 mg/l)

Table 5: BDST model parameters for the adsorption of Cu (II) on raw melon husk in a fixed bed column

Q(ml/min)	C <sub>0</sub> (mg/l)	K(Lmg <sup>-1</sup> min <sup>-1</sup> )	N <sub>0</sub> (mg/l)	R <sup>2</sup>
0.5	5	-0.001	0.773	0.991

#### 4. CONCLUSION

Experimental fixed bed column adsorption study and theoretical modelling of Cu (II) ion removal from aqueous solution using melon (*Citrus cocolynthus*) husk was studied. The findings showed that raw melon husk is a potential effective and economically viable biosorbent for the removal of Cu (II) ion from aqueous solution evident from the high % metal removal achieved. FT-IR characterization of the melon husk showed that it is a complex material having several peaks whose major functional groups (carboxylic and amine groups) changes position which can be deduced to be the points of Cu ((II) ion attachment to the adsorbent surface. SEM study revealed the melon husk high surface area whose porosity decreases as it adsorbs metal ions. Though, adsorbent bed did not attain saturation after 4900 minutes, interactions between the operating parameters was investigated and the responses determined were established which shows the adsorption capacity dependence on the bed height, initial copper (II) ions concentration and flow rate. The maximum column sorption capacity, % removal and equilibrium uptake decreased with increased flow rate but increased with increased bed height. The initial metal concentration also favours an increase in sorption capacity and equilibrium uptake but at a reduced volume of treated solution. The low flow rate provided more residence time for intimate contact and higher bed heights and initial metal concentration means more sorption sites and higher transfer gradients are made available for an effective metal (Cu (II) ion) removal. Though, the column performance indicators had shown the potentials of the column adsorption of Cu (II) on raw melon husk but the models used could not adequately describe the breakthrough curves except the BDST model whose correlation of 0.991 indicated a good agreement between the theoretical prediction and the experimental data. High correlation coefficient of  $R^2 = 0.991$  showed that the variation of the service time with the bed depth was highly linear for all the systems, thus, indicating the validity of the BDST model when applied to the continuous column studies.

#### 5. ACKNOWLEDGMENT

The authors wish to acknowledge the assistance and contributions of the laboratory staff of Department of Chemical Engineering, Federal University of Technology Minna.

## 6. CONFLICT OF INTEREST

There is no conflict of interest associated with this work.

## REFERENCES

- Abdolali, A., Ngo, H.H., Guo, W., Lu, S., Chen, S., Nguyen, N.C., Zhang, X., Wang, J. and Wu Y. (2016). A breakthrough biosorbent in removing heavy metals: Equilibrium, kinetic, thermodynamic and mechanism analyses in a lab-scale study. *Science of the Total Environment*, 542, pp. 603–611.
- Ahmad, M.F., Haydar, S. and Ahmad (2016). Evaluation of a newly developed biosorbent using packed bed column for possible application in the treatment of industrial effluents for removal of cadmium ions. *Journal of the Taiwan Institute of Chemical Engineers*, 62, pp. 122-123.
- Ajmal, M., Khan, A.H., Ahmad, S. and Ahmad A. (1998). Role of sawdust in the removal of copper (II) from industrial wastes *Water Resources*, 32, pp. 3085-3091.
- Alyüz B., Veli S. (2009). Kinetics and equilibrium studies for the removal of nickel and zinc from aqueous solutions by ion exchange resins. *Journal of Hazardous Material*, 167, pp. 482-488.
- Amirnia S., Ray M.B., Margaritis A. (2016). Copper ion removal by *Acer saccharum* leaves in a regenerable continuous-flow column. *Chemical Engineering Journal*, 287, pp. 755–764.
- Asadi, F., Shariatmadari, H., Mirghaffari, N. (2008). Modification of rice hull and sawdust sorptive characteristics for remove heavy metals from synthetic solutions and wastewater. *Journal of Hazardous Materials*, 154, pp.451–458.
- Babarinde A. and Omisore G. (2014). Application of kinetic, isothermal and thermodynamic models in the biosorption of Cd (II), Pb (II) and Zn (II) from solutions onto Melon (*Citrullus Lanatus*) seed husks. *International Journal of Chemical and Biochemical Sciences, IJCBS*, 5, pp. 72-85.
- Basu M., Guha A., Ray L. (2017). Adsorption of Lead on Cucumber Peel. *Journal of Cleaner Production*, 151, pp. 603-615.
- Blanes P.S, Bordoni M.E., González J.C., García S.I., Atria A.M., Sala L.F., Bellú S.E. (2016). Application of soy hull biomass in removal of Cr (VI) from contaminated waters. Kinetic, thermodynamic and continuous sorption studies. *Journal of Environmental Chemical Engineering*, 4, pp. 516-526.
- Chaundry, H. and Ijaz, M. (2014). Removal of lead from Wastewater by Adsorption on saponified Melon peel. *Geology Science International (Lahore)*, 26(2), pp. 705-708.
- Chellam, G.A., Shakina, J., and Usha, R. (2014). Studies of the adsorption of Cadmium (II) on Cucumis melon peel. *Indian journal of science*, 2(22), pp. 72-85.
- Choong C., Ibrahim S., Yoon Y., Jang M. (2018). Removal of lead and bisphenol A using magnesium silicate impregnated palm-shell waste powdered activated carbon: comparative studies on single and binary pollutant adsorption. *Ecotoxicity and Environmental safety*. 148, pp. 142-151.
- Chowdhury Z. Z., Zain S. M., Rashid A. K., Rafique R. F., Khalid K. (2013). Breakthrough Curve Analysis for Column Dynamics Sorption of Mn (II) Ions from Wastewater by Using *Mangostana garcinia* Peel-Based Granular-Activated Carbon. *Journal of Chemistry*, 2013, pp. 1-8.
- Daniel O.O., Chima E.S., Chinedu M.T. (2014). Comparative study on the bioadsorption of cadmium and lead from industrial waste water using activated melon (*citrullus colocynthis*) husk activated with sulphuric acid. *American Journal of Environmental Protection*, 3(6-1), pp. 1-8.
- Djelloul C., Hamdaoui O. (2014). Dynamic adsorption of methylene blue by melon peel in fixed-bed columns. *Desalination and water Treatment*, pp. 1-10.
- Foo K. Y. and Hameed B. H. (2012). Preparation and Characterization of Activated Carbon from melon (*Citrullus Vulgaris*) Seed Hull by Microwave-induced NaOH Activation. *Desalination and Water Treatment*, 47:1-3, pp. 130-138.
- Ghasemi M., Naushad M., Ghasemi N., Khosravi-fard Y. (2014). Adsorption of Pb(II) from aqueous solution using new adsorbents prepared from agricultural waste: adsorption isotherm and kinetic studies. *Journal of industrial and Engineering. Chemistry*. 20(4) pp. 2193-219

- Giwa, A.A., Bello, I.A., Oladipo, M.A. and Adeoye, R.O. (2013). Removal of Cadmium from wastewater by Adsorption using husk of melon (*Citrullus lanatus*) seed. *International Journal of Basic and Applied Science*. Vol. 02, No. 01, pp. 110-123.
- Gupta, V.K. (2003). Removal of cadmium and nickel from wastewater using bagasse fly ash-a sugar industry waste. *Water Resources* 37(16), pp. 4038-44.
- Kanadasan, G., Mashitah, M.D. (2010). Fixed bed adsorption of methylene blue by using palm oil mill effluent waste activated sludge. School of Chemical Engineering, Universiti Sains Malaysia, available at <https://core.ac.uk/download/pdf/11969455.pdf>.
- Kausar A., Bhatti H., Mackinnon G. (2016). Reuse of agricultural wastes for the removal and recovery of Zr (IV) from aqueous solution. *Journal of the Taiwan institute of chemical engineering*, 59, pp. 330-340.
- Lodeiro P., Herrero R., Sastre de Vicente M.E (2006). The use of protonated *Sargassum muticum* as biosorbent for cadmium removal in a fixed-bed column. *Journal of Hazardous Materials*, B137, pp. 244-253
- Malkoc E., Nuhoglu Y. (2006). Removal of Ni (II) ions from aqueous solutions using waste of tea factory: Adsorption on a fixed-bed column. *Journal of Hazardous Materials*, B135, pp. 328-336.
- Markou G, Mitrogiannis D, Muylaert K, Çelekli A, Bozkurt H. (2016). Biosorption and retention of orthophosphate onto Ca(OH)<sub>2</sub>-pretreated biomass of *Phragmites* sp. *Journal of Environmental Sciences*, 45, pp 49-59.
- Martín-Lara M.A., Blázquez G., Calero M., Almendros A.I., Ronda A. (2016). Binary biosorption of copper and lead onto pine cone shell in batch reactors and in fixed bed columns. *International Journal of Mineral Processing*, 148, pp. 72–82.
- Mousumi, B., Arun, K. and Lalitagauri, R. (2017). Adsorption of lead on cucumber peel. *Journal. of cleaner production*. 151, pp. 603-615.
- Muhammad, A.A., Mahmood, K and Abdul, W. (2011). Study of low cost biosorbent for biosorption of heavy metals. *International Conference on Food Engineering and Biotechnology (IPCBBE)*, 9, pp. 60-68.
- Nasehir, K., Yahaya, M.E., Ismail, A., Muhammad, F.P and Mohammed, L. (2011) Fixed-bed Column Study for Cu (II) Removal from Aqueous Solutions using Rice Husk based Activated Carbon. *International Journal of Engineering & Technology* 11(1), pp. 8704-3434.
- Nwabanne J.T. and Igbokwe, P.K. (2012). Kinetic Modeling of Heavy Metals Adsorption on fixed bed Column. *International Journal on Environmental. Resources*. 6(4), pp. 945-952.
- Nwankwo, M.O. (2007). A comparative study on the bio adsorption of cadmium and lead from industrial waste water using activated melon (*Citrullus colocynthis*) husk, MSc. Thesis, Nnamdi Azikiwe University Awka, Nigeria.
- Panda G.C., Das S.K., Bandyopadhyay T.S., Guha A.K. (2007). Adsorption of nickel on husk of *Lathyrus sativus*: behaviour and binding mechanism. *Colloids and surfaces B: Biointerfaces*, 57, pp. 135-142.
- Reddy N., Lakshmi pathy R., Sarada N. (2014). Application of *Citrullus lanatus* rind as biosorbent for removal of trivalent chromium from aqueous solution, 53, pp. 969-975.
- Saad D.M., Cukrowska E., Tutu H. (2015). Column adsorption studies for the removal of U by phosphonated cross-linked polyethylenimine: modelling and optimization. *Applied Water Science*, Volume 5, Issue 1, pp. 57-63.
- Saeedeh, H., Khatereh S., Zahra Y. (2014). Preparation of activated carbon from agricultural wastes (almond shell and orange peel) for adsorption of 2-pic from aqueous solution. *Journal of industrial and Engineering Chemistry*, 20, pp. 1892-1900.
- Shekhula M.M., Okonkwo O.J., Zvinowanda C.M., Agyel N.N., Chaudhary A.J. (2012). Fixed bed Column Adsorption of Cu (II) onto Maize Tassel-PVA Beads. *Journal of Chemical Engineering Process Technology*, 3:2, pp. 1-5.
- Sivakumar P., Palanisamy P.N. (2009). Packed bed column studies for the removal of Acid Blue 92 and Basic red 29 using non-conventional adsorbent. *Indian Journal of Chemical technology*, 16, pp. 301-307.
- Sunday, A.L., Imtiaz, A.C and Yusoff, N. (2012). An assessment of the physio-chemical properties of melon seed (*Citrullus lanatus*) oil as a base material for oil-in-water emulsion cutting fluid. *Advanced materials Research*, Vol. 576, pp. 293-295.
- Taty-Costodes V.C., Fauduet H., Porte C., Ho Y. (2005). Removal of lead (II) ions from synthetic and real effluents using immobilized *Pinus sylvestris* sawdust: Adsorption on a fixed-bed column. *Journal of Hazardous Materials*, B123, pp. 135-144.

- Ushakumary, E.R and Madhu, G. (2014) Studies on Zinc (II) Adsorption Using *Alisma Plantago Aquatica*. *Journal of Clean Energy Technologies*, Vol. 2, No. 2.
- Vijayaraghavan, K. and Yun, Y.S. (2008) Bacterial biosorbents and biosorption. *Biotechnology. Advancement*, 26, pp. 266-291.
- Watwoyo W, Seo CW, Marshall W.E. (1999). Utilization of peanut shells as adsorbents for selected metals. *Journal of Chemical Technology Biotechnology*, 74, pp. 1117-21.
- Wong K.K., Lee C.K., Low K.S., Haron M.J. (2003). Removal of Cu and Pb from electroplating wastewater using tartaric acid modified rice husk. *Process biochemistry*, 39, pp. 37-445.
- Yahya, M.D and Odigure, J.O. (2015). Fixed bed column study for Pb (II) adsorption using calcium-alginate treated shea butter husk (TSBH). In: Book of Proceeding of International Conference on Industrial Engineering and Operations Management, Dubai, UAE. ID-724.
- Yahya, M.D. Mohammed-Dabo, I.A. Ahmed, A.S. Olawale, A.S. (2013). Adsorptive removal of Lead from aqueous solution using Raw Shea Butter Cake (RSBC) and Modified Shea Butter Cake (MSBC). *Journal of Nigeria Society of Chemical Engineers*, 28 (1), pp. 25-33.
- Zhang J., Fu H., Lv X., Tang J., Xu X (2011). Removal of Cu (II) from aqueous solution using rice husk carbons prepared by the physical activation process. *Biomass and Bioenergy*, 35, pp. 464-472.
- Zulkali M.M.D., Ahmad A.L., Norulakmal N.H. (2006). *Oryza sativa* L. husk as heavy metal adsorbent: Optimization with lead as model. *Bioresource Technology*, 97(1) pp. 21-25.